

# Double-Diffusive Mixed Convection in a Porous Open Cavity Filled with a Nanofluid Using Buongiorno's Model

M. A. Sheremet<sup>1,2</sup> · I. Pop<sup>3</sup> · A. Ishak<sup>4</sup>

Received: 22 December 2014 / Accepted: 29 April 2015 / Published online: 10 May 2015  
© Springer Science+Business Media Dordrecht 2015

**Abstract** This work examines the steady double-diffusive mixed convection flow in a porous open cavity filled with a nanofluid using mathematical nanofluid model proposed by Buongiorno. The analysis uses a two-dimensional square cavity of size  $L$  with an inlet of size  $0.2 \cdot L$  in the bottom part of the left vertical wall and an outlet of the same size in the upper part of the right vertical wall. The mathematical problem is represented by non-dimensional governing equations along with the corresponding boundary conditions, which are solved numerically using a second-order accurate finite difference method. The developed algorithm has been validated by direct comparisons with previously published papers, and the results have been found to be in good agreement. Particular efforts have been focused on the effects of the key parameters on the fluid flow, heat and mass transfer characteristics. In addition, numerical results for the average Nusselt and Sherwood numbers are presented in tabular forms for various parametric conditions and discussed.

**Keywords** Double-diffusive · Mixed convection · Square cavity · Porous media · Nanofluids · Numerical method

---

✉ I. Pop  
popm.ioan@yahoo.co.uk

M. A. Sheremet  
michael-sher@yandex.ru

A. Ishak  
anuarishak@yahoo.com

<sup>1</sup> Department of Theoretical Mechanics, Faculty of Mechanics and Mathematics, Tomsk State University, 634050 Tomsk, Russia

<sup>2</sup> Institute of Power Engineering, Tomsk Polytechnic University, 634050 Tomsk, Russia

<sup>3</sup> Department of Applied Mathematics, Babeş-Bolyai University, 400084 Cluj-Napoca, Romania

<sup>4</sup> School of Mathematical Sciences, Faculty of Science and Technology, Universiti Kebangsaan Malaysia (UKM), 43600 Bangi, Selangor, Malaysia

## 1 Introduction

Convective flow in cavities filled with porous media is a topic of fundamental heat transfer in many analyses and has received considerable attention over the last few decades. This interest is due to its wide range of applications, for example, high-performance insulation for buildings, chemical catalytic reactors, packed sphere beds, grain storage, float glass production, air-conditioning in rooms, cooling of electronic devices, and such geophysical problems as frost heave (Kaviany 1999; Nield and Bejan 2013; Saleh and Hashim 2013).

It has been shown by Mohamad (1995) that natural convection in open cavities has received much attention due to the importance of such geometry in solar thermal receiver systems, fire research, electronic cooling devices, energy-saving household refrigerators, etc. Further, Bilgen and Oztop (2005) pointed out that partially open cavities are encountered in various engineering systems, uncovered flat plate solar collectors having rows of vertical strips, in buildings, etc. In these situations, the flow may be substantially affected by the flow at the openings. The spread and growth of the combustion products in a room, for example, are substantially governed by the location and size of the doors and windows (Abib and Jaluria 1988).

It is well established (see De Groot and Mazur 1984) that a multicomponent system under non-isothermal condition is subject to mass transfer related to coupled-transport phenomena. This has strong practical importance in many situations since the flow dynamics and convective patterns in mixtures are more complex than those of one-component fluids due to the interplay between advection and mixing, solute diffusion (see Davarzani et al. 2010). There are many important processes in nature and technology where thermal diffusion plays a crucial role. It has various technical applications, such as isotope separation in liquid and gaseous mixtures (see Rabinovich 1981), polymer solutions and colloidal dispersions (see Wiegand 2004), study of compositional variation in hydrocarbon reservoirs (see Firoozabadi 1991), and coating of metallic items. It also affects component separation in oil wells, solidifying metallic alloys, volcanic lava, and in the Earth Mantle (see Ilya 2006).

The double-diffusive convection in a porous cavity has been studied by several researchers. Goyeau et al. (1996) considered the double-diffusive natural convection in a porous cavity using Darcy-Brinkman formulation. Karimi-Fard et al. (1997) investigated the non-Darcian effects on double-diffusive natural convection within a porous square cavity filled with a porous media. At the same time, Nithiarasu et al. (1997) considered the double-diffusive natural convection in a fluid-saturated porous cavity with a freely convecting wall. Bennacer et al. (2001) considered the problem of the double-diffusive natural convection in a vertical enclosure filled with anisotropic porous medium. The problem of double-diffusive convection in inclined triangular porous enclosures with sinusoidal variation of boundary conditions was discussed numerically by Mansour et al. (2011). Finally, we mention the paper by Rashad et al. (2014) (who has studied the effects of chemical reaction and thermal radiation on unsteady double-diffusive convection in a square enclosure filled with a porous medium with sinusoidal boundary conditions on the bottom wall).

It is already well known that ultrahigh-performance cooling is one of the most vital needs of many industrial technologies. However, inherently low thermal conductivity is a primary limitation in developing energy-efficient heat transfer fluids that are required for ultrahigh-performance cooling. Because of the increasing necessity of the modern technology, including chemical processes, microelectronics, biotechnology, etc., it is very important to obtain new type of fluids, having improved heat transfer characteristics. In order to enhance the thermal characteristics of the fluids, one can form mixtures by adding ultrafine solid particles (metallic, nonmetallic or polymeric) to the fluid. Nanofluids technology, a new interdisciplinary field

of great importance, where nanoscience, nanotechnology, and thermal engineering meet, has largely developed over the past several decades. Nanofluids are new types of fluids containing small fractions of nanoparticles, usually smaller than 100 nm, which are uniformly and stable suspended in a liquid. The thermal behavior of nanofluids provides a basis for heat transfer intensification, in industrial sectors including power generation, thermal therapy for cancer treatment, chemical sectors, ventilation, refrigeration, etc. It is also mentioned in the book by Schaefer (2010) that from the top ten advances in materials science, at least five are directly related to nanoscience, such as materials science, information processing, biotechnology, chemistry, and medicine. In biological systems, nanosized structures play an important role from proteins to deoxyribonucleic acid carrying the genetic code, ribonucleic acid.

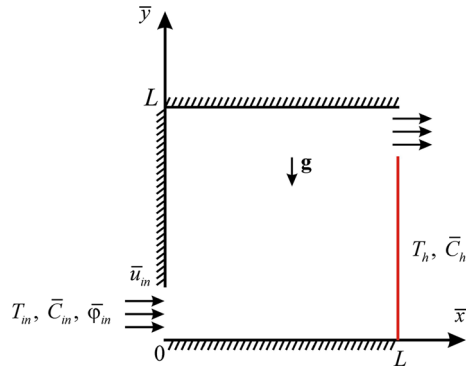
Buongiorno (2006) developed a non-homogeneous equilibrium model by considering the effect of the Brownian diffusion and thermophoresis that are important slip mechanisms in nanofluid. This model has been widely used by many researchers to study the free convection boundary layer flow past a vertical flat plate embedded in a porous medium filled by nanofluids (Nield and Kuznetsov 2011; Kuznetsov and Nield 2011) or flow and heat transfer over a stretching/shrinking surface (Khan and Pop 2010; Bachok et al. 2011), etc.

In the present study, we investigate the double-diffusive mixed convection in a porous open cavity filled with a nanofluid using the mathematical nanofluid model proposed by Buongiorno (2006). The Darcy model is used in the porous layer. It should be mentioned that many researchers focused their studies on effects of aspect ratios on the double-diffusive natural convection in enclosures. Chamkha and Al-Naser (2001) studied the unsteady laminar double-diffusive convective flow in an inclined rectangular enclosure filled with a uniform porous medium. Costa (2004a) studied the double-diffusive natural convections in parallelogrammic enclosures, and emphasis was given to the situation that the porous media in the enclosure were saturated with moist air. The same author (Costa 2004b) also pointed out that the combinations of different aspect ratios and inclination angles can lead to considerably high heat and mass transfer rates in the enclosure. Further, we mention that Jeng et al. (2009) performed the experimental and numerical studies of the transient natural convection due to mass transfer in the inclined enclosures at different inclination angles. The Rayleigh number  $Ra$  ranged from  $1.126 \times 10^8$  to  $1.157 \times 10^{11}$  and the angle of inclination  $\varphi$  varied from 30 to 90°; the aspects ratio of the enclosure  $A$  was changed from 0.6 to 1.

## 2 Basic Equations

Figure 1 shows the considered double-diffusive mixed convection flow, heat and mass transfer in a porous open cavity filled with a water based nanofluid. It is assumed that nanoparticles are suspended in the nanofluid using either surfactant or surface charge technology. This prevents nanoparticles from agglomeration and deposition on the porous matrix (see Nield and Kuznetsov 2011; Kuznetsov and Nield 2011). The porous medium is assumed to be homogeneous and isotropic, and the local thermal equilibrium is valid. The flow in the cavity is considered to be steady, laminar, and incompressible. The domain of interest is a square cavity of size  $L$  with an inlet of size  $0.2 \cdot L$  in the bottom part of the left vertical wall and an outlet of the same size in the upper part of the right vertical wall. The heat source of high temperature  $T_h$  and a contaminant source of high concentration  $\bar{C}_h$  are considered on the right vertical wall. The rest of the walls of the cavity are assumed to be adiabatic and impermeable. In addition, the incoming nanofluid through the inlet with nanoparticle volume fraction  $\bar{\varphi}_{in}$  is at a uniform horizontal velocity  $\bar{u}_{in}$  ( $\bar{v}_{in} = 0$ ) at the constant ambient temperature  $T_{in}$  and concentration  $\bar{C}_{in}$ .

**Fig. 1** Physical model and coordinate system



It should be noted that we investigate in this paper the interaction between base fluid, nanoparticles, and porous structure when the base fluid of nanofluid is a binary fluid such as salty water. The outcome is that we are studying a sort of triple-diffusion problem in a porous structure involving heat, the nanoparticles and the contaminant. As suggested by one Reviewer, there should be a net throughflow through the cavity, so that there will be an extra contribution to the nanoparticle flux (see [Jaimala and Singh 2014](#); [Nield and Kuznetsov 2015](#)). Thus, the basic equations for the flow, heat transfer, contaminant and nanoparticles transport can be written in the following form (see [Jaimala and Singh 2014](#), and [Nield and Kuznetsov 2015](#)).

$$\nabla \cdot \mathbf{V} = 0 \tag{1}$$

$$\frac{\rho_{f0}}{\varepsilon} \frac{\partial \mathbf{V}}{\partial t} = -\nabla p - \frac{\mu}{K} \mathbf{V} + [\bar{\varphi} \rho_p + (1 - \bar{\varphi}) \{ \rho_{f0} (1 - \beta_T (T - T_{in}) - \beta_C (\bar{C} - \bar{C}_{in})) \}] \mathbf{g} \tag{2}$$

$$(\rho C_p)_m \frac{\partial T}{\partial t} + (\rho C_p)_f (\mathbf{V} \cdot \nabla) T = \nabla (k_m \nabla T) + \varepsilon (\rho C_p)_p \left[ D_B \nabla \bar{\varphi} \cdot \nabla T + (D_T/T_c) \nabla T \cdot \nabla T - \frac{(\bar{\varphi} - \bar{\varphi}_{in})}{\varepsilon} \mathbf{V} \cdot \nabla T \right] + (\rho C_p)_m \nabla (D_{TC} \nabla \bar{C}) \tag{3}$$

$$\frac{\partial \bar{C}}{\partial t} + \frac{1}{\varepsilon} (\mathbf{V} \cdot \nabla) \bar{C} = \nabla [D_{Sm} \nabla \bar{C} + D_{CT} \nabla T] \tag{4}$$

$$\frac{\partial \bar{\varphi}}{\partial t} + \frac{1}{\varepsilon} (\mathbf{V} \cdot \nabla) \bar{\varphi} = \nabla [D_B \nabla \bar{\varphi} + (D_T/T_c) \nabla T] \tag{5}$$

where  $\mathbf{V}$  is the Darcy velocity vector,  $T$  is the fluid temperature,  $\bar{C}$  is the contaminant concentration,  $\bar{\varphi}$  is the nanoparticle volume fraction,  $t$  is the time,  $p$  is the fluid pressure,  $\mathbf{g}$  is the gravity vector,  $\varepsilon$  is the porosity of the porous medium,  $K$  is the permeability of the porous medium,  $\rho_{f0}$  is the reference density of the fluid,  $\mu$  is the viscosity of the fluid,  $\beta_T$  is the thermal expansion coefficient,  $\beta_C$  is the contaminant expansion coefficient,  $\rho_p$  is the nanoparticle mass density,  $(\rho C_p)_f$  is the volume heat capacity of the fluid,  $(\rho C_p)_m$  is the effective volume heat capacity of the porous medium,  $k_m$  is the effective thermal conductivity of the porous medium,  $(\rho C_p)_p$  is the effective volume heat capacity of the nanoparticle material,  $D_B$  is the Brownian diffusion coefficient,  $D_T$  is the thermophoretic diffusion coefficient,  $D_{TC}$  is the diffusivity of Dufour type,  $D_{Sm}$  is the contaminant diffusivity for the porous medium, and  $D_{CT}$  is the diffusivity of Soret type. It should be mentioned that we

have neglected here the term  $k_d \nabla T$ , where  $k_d$  is the enhancement in the thermal conductivity due to the thermal dispersion (see [Khanafer et al. 2003](#) and [Nakayama 1995](#)). This is because we have used the model proposed by [Buongiorno \(2006\)](#), and [Nield and Kuznetsov \(2015\)](#). But, in the future work, we will take into account this phenomenon in order to evaluate this mechanism in comparison with other ones.

The flow is assumed to be slow so that an advective term and a Forchheimer quadratic drag term do not appear in the momentum equation. It is assumed also that the contaminant does not affect the transport of the nanoparticles. In keeping with the Boussinesq approximation and an assumption that the nanoparticle concentration is dilute, and with a suitable choice for the reference pressure, we can linearize the momentum equation and write Eq. (2) as

$$0 = -\nabla p - \frac{\mu}{K} \mathbf{V} + [\bar{\varphi} (\rho_p - \rho_{f0}) + \rho_{f0} (1 - (1 - \bar{\varphi}_{in}) \{ \beta_T (T - T_{in}) + \beta_C (\bar{C} - \bar{C}_{in}) \})] \mathbf{g} \tag{6}$$

Equations (1), (3)–(6) for the steady problem under consideration can be written in dimensional coordinates  $\bar{x}, \bar{y}$  as follows

$$\frac{\partial \bar{u}}{\partial \bar{x}} + \frac{\partial \bar{v}}{\partial \bar{y}} = 0 \tag{7}$$

$$\frac{\partial p}{\partial \bar{x}} = -\frac{\mu}{K} \bar{u} \tag{8}$$

$$\frac{\partial p}{\partial \bar{y}} = -\frac{\mu}{K} \bar{v} - [\bar{\varphi} (\rho_p - \rho_{f0}) + \rho_{f0} (1 - (1 - \bar{\varphi}_{in}) \{ \beta_T (T - T_{in}) + \beta_C (\bar{C} - \bar{C}_{in}) \})] g \tag{9}$$

$$\begin{aligned} \bar{u} \frac{\partial T}{\partial \bar{x}} + \bar{v} \frac{\partial T}{\partial \bar{y}} &= \alpha_m \left( \frac{\partial^2 T}{\partial \bar{x}^2} + \frac{\partial^2 T}{\partial \bar{y}^2} \right) + \delta \left\{ D_B \left( \frac{\partial \bar{\varphi}}{\partial \bar{x}} \frac{\partial T}{\partial \bar{x}} + \frac{\partial \bar{\varphi}}{\partial \bar{y}} \frac{\partial T}{\partial \bar{y}} \right) \right. \\ &\quad \left. - \frac{(\bar{\varphi} - \bar{\varphi}_{in})}{\varepsilon} \left( \bar{u} \frac{\partial T}{\partial \bar{x}} + \bar{v} \frac{\partial T}{\partial \bar{y}} \right) + \frac{D_T}{T_c} \left[ \left( \frac{\partial T}{\partial \bar{x}} \right)^2 + \left( \frac{\partial T}{\partial \bar{y}} \right)^2 \right] \right\} + \sigma D_{TC} \left( \frac{\partial^2 \bar{C}}{\partial \bar{x}^2} + \frac{\partial^2 \bar{C}}{\partial \bar{y}^2} \right) \end{aligned} \tag{10}$$

$$\frac{1}{\varepsilon} \left( \bar{u} \frac{\partial \bar{C}}{\partial \bar{x}} + \bar{v} \frac{\partial \bar{C}}{\partial \bar{y}} \right) = D_{Sm} \left( \frac{\partial^2 \bar{C}}{\partial \bar{x}^2} + \frac{\partial^2 \bar{C}}{\partial \bar{y}^2} \right) + D_{CT} \left( \frac{\partial^2 T}{\partial \bar{x}^2} + \frac{\partial^2 T}{\partial \bar{y}^2} \right) \tag{11}$$

$$\frac{1}{\varepsilon} \left( \bar{u} \frac{\partial \bar{\varphi}}{\partial \bar{x}} + \bar{v} \frac{\partial \bar{\varphi}}{\partial \bar{y}} \right) = D_B \left( \frac{\partial^2 \bar{\varphi}}{\partial \bar{x}^2} + \frac{\partial^2 \bar{\varphi}}{\partial \bar{y}^2} \right) + \frac{D_T}{T_{in}} \left( \frac{\partial^2 T}{\partial \bar{x}^2} + \frac{\partial^2 T}{\partial \bar{y}^2} \right) \tag{12}$$

where  $\bar{u}, \bar{v}$  are the velocity components along  $\bar{x}, \bar{y}$  directions, respectively.

One can introduce a stream function  $\bar{\psi}$  defined by

$$\bar{u} = \frac{\partial \bar{\psi}}{\partial \bar{y}}, \quad v = -\frac{\partial \bar{\psi}}{\partial \bar{x}} \tag{13}$$

so that Eq. (7) is satisfied identically. We are then left with the following equations

$$\frac{\partial^2 \bar{\psi}}{\partial \bar{x}^2} + \frac{\partial^2 \bar{\psi}}{\partial \bar{y}^2} = \frac{\rho_p - \rho_{f0}}{\mu} K g \frac{\partial \bar{\varphi}}{\partial \bar{x}} - \frac{\rho_{f0} g \beta_T (1 - \bar{\varphi}_{in}) K}{\mu} \frac{\partial T}{\partial \bar{x}} - \frac{\rho_{f0} g \beta_C (1 - \bar{\varphi}_{in}) K}{\mu} \frac{\partial \bar{C}}{\partial \bar{x}} \tag{14}$$

$$\begin{aligned} \frac{\partial \bar{\psi}}{\partial \bar{y}} \frac{\partial T}{\partial \bar{x}} - \frac{\partial \bar{\psi}}{\partial \bar{x}} \frac{\partial T}{\partial \bar{y}} &= \alpha_m \left( \frac{\partial^2 T}{\partial \bar{x}^2} + \frac{\partial^2 T}{\partial \bar{y}^2} \right) + \delta \left\{ D_B \left( \frac{\partial \bar{\varphi}}{\partial \bar{x}} \frac{\partial T}{\partial \bar{x}} + \frac{\partial \bar{\varphi}}{\partial \bar{y}} \frac{\partial T}{\partial \bar{y}} \right) \right. \\ &\quad \left. - \frac{(\bar{\varphi} - \bar{\varphi}_{in})}{\varepsilon} \left( \frac{\partial \bar{\psi}}{\partial \bar{y}} \frac{\partial T}{\partial \bar{x}} - \frac{\partial \bar{\psi}}{\partial \bar{x}} \frac{\partial T}{\partial \bar{y}} \right) + \frac{D_T}{T_c} \left[ \left( \frac{\partial T}{\partial \bar{x}} \right)^2 + \left( \frac{\partial T}{\partial \bar{y}} \right)^2 \right] \right\} \\ &\quad + \sigma D_{TC} \left( \frac{\partial^2 \bar{C}}{\partial \bar{x}^2} + \frac{\partial^2 \bar{C}}{\partial \bar{y}^2} \right) \end{aligned} \tag{15}$$

$$\frac{1}{\varepsilon} \left( \frac{\partial \bar{\psi}}{\partial \bar{y}} \frac{\partial \bar{C}}{\partial \bar{x}} - \frac{\partial \bar{\psi}}{\partial \bar{x}} \frac{\partial \bar{C}}{\partial \bar{y}} \right) = D_{Sm} \left( \frac{\partial^2 \bar{C}}{\partial \bar{x}^2} + \frac{\partial^2 \bar{C}}{\partial \bar{y}^2} \right) + D_{CT} \left( \frac{\partial^2 T}{\partial \bar{x}^2} + \frac{\partial^2 T}{\partial \bar{y}^2} \right) \tag{16}$$

$$\frac{1}{\varepsilon} \left( \frac{\partial \bar{\psi}}{\partial \bar{y}} \frac{\partial \bar{\varphi}}{\partial \bar{x}} - \frac{\partial \bar{\psi}}{\partial \bar{x}} \frac{\partial \bar{\varphi}}{\partial \bar{y}} \right) = D_B \left( \frac{\partial^2 \bar{\varphi}}{\partial \bar{x}^2} + \frac{\partial^2 \bar{\varphi}}{\partial \bar{y}^2} \right) + \frac{D_T}{T_{in}} \left( \frac{\partial^2 T}{\partial \bar{x}^2} + \frac{\partial^2 T}{\partial \bar{y}^2} \right) \tag{17}$$

Introducing the following dimensionless variables

$$\begin{aligned} x &= \bar{x}/L, \quad y = \bar{y}/L, \quad \psi = \bar{\psi}/\alpha_m, \quad \theta = (T - T_{in})/(T_h - T_{in}), \\ C &= (\bar{C} - \bar{C}_{in})/(\bar{C}_h - \bar{C}_{in}), \quad \varphi = \bar{\varphi}/\bar{\varphi}_{in} \end{aligned} \tag{18}$$

and substituting (18) into Eqs. (14)–(17), we obtain

$$\frac{\partial^2 \psi}{\partial x^2} + \frac{\partial^2 \psi}{\partial y^2} = -Ra \left( \frac{\partial \theta}{\partial x} + Nc \frac{\partial C}{\partial x} - Nr \frac{\partial \varphi}{\partial x} \right) \tag{19}$$

$$\begin{aligned} \frac{\partial \psi}{\partial y} \frac{\partial \theta}{\partial x} - \frac{\partial \psi}{\partial x} \frac{\partial \theta}{\partial y} &= \frac{\partial^2 \theta}{\partial x^2} + \frac{\partial^2 \theta}{\partial y^2} + Nb \left( \frac{\partial \varphi}{\partial x} \frac{\partial \theta}{\partial x} + \frac{\partial \varphi}{\partial y} \frac{\partial \theta}{\partial y} \right) \\ &\quad + (1 - \varphi) Nb \cdot Ln \left( \frac{\partial \psi}{\partial y} \frac{\partial \theta}{\partial x} - \frac{\partial \psi}{\partial x} \frac{\partial \theta}{\partial y} \right) + Nt \left[ \left( \frac{\partial \theta}{\partial x} \right)^2 + \left( \frac{\partial \theta}{\partial y} \right)^2 \right] + Nd \left( \frac{\partial^2 C}{\partial x^2} + \frac{\partial^2 C}{\partial y^2} \right) \end{aligned} \tag{20}$$

$$\frac{\partial \psi}{\partial y} \frac{\partial C}{\partial x} - \frac{\partial \psi}{\partial x} \frac{\partial C}{\partial y} = \frac{1}{Le} \left( \frac{\partial^2 C}{\partial x^2} + \frac{\partial^2 C}{\partial y^2} \right) + \frac{Ld}{Le} \left( \frac{\partial^2 \theta}{\partial x^2} + \frac{\partial^2 \theta}{\partial y^2} \right) \tag{21}$$

$$\frac{\partial \psi}{\partial y} \frac{\partial \varphi}{\partial x} - \frac{\partial \psi}{\partial x} \frac{\partial \varphi}{\partial y} = \frac{1}{Ln} \left( \frac{\partial^2 \varphi}{\partial x^2} + \frac{\partial^2 \varphi}{\partial y^2} \right) + \frac{Nt}{Ln \cdot Nb} \left( \frac{\partial^2 \theta}{\partial x^2} + \frac{\partial^2 \theta}{\partial y^2} \right) \tag{22}$$

The corresponding boundary conditions for these equations are as follows (see [Kuznetsov and Nield 2013](#))

$$\begin{aligned} \psi &= Re \cdot Pr \cdot 0.2, \quad \frac{\partial \theta}{\partial x} = 0, \quad \frac{\partial C}{\partial x} = 0, \quad \frac{\partial \varphi}{\partial x} = 0 \quad \text{on } x = 0, \quad 0.2 \leq y < 1 \\ \psi &= Re \cdot Pr \cdot y, \quad \theta = 0, \quad C = 0, \quad \varphi = 1 \quad \text{on } x = 0, \quad 0 < y < 0.2 \\ \psi &= 0, \quad \theta = 1, \quad C = 1, \quad Nb \frac{\partial \varphi}{\partial x} + Nt \frac{\partial \theta}{\partial x} = 0 \quad \text{on } x = 1, \quad 0 < y \leq 0.8 \\ \frac{\partial \psi}{\partial x} &= 0, \quad \frac{\partial \theta}{\partial x} = 0, \quad \frac{\partial C}{\partial x} = 0, \quad \frac{\partial \varphi}{\partial x} = 0 \quad \text{on } x = 1, \quad 0.8 < y < 1 \\ \psi &= 0, \quad \frac{\partial \theta}{\partial y} = 0, \quad \frac{\partial C}{\partial y} = 0, \quad \frac{\partial \varphi}{\partial y} = 0 \quad \text{on } y = 0 \\ \psi &= Re \cdot Pr \cdot 0.2, \quad \frac{\partial \theta}{\partial y} = 0, \quad \frac{\partial C}{\partial y} = 0, \quad \frac{\partial \varphi}{\partial y} = 0 \quad \text{on } y = 1 \end{aligned} \tag{23}$$

Here  $Re$  is the Reynolds number,  $Pr$  is the Prandtl number for the porous medium,  $Ra$  is the Rayleigh number for the porous media,  $Nr$  is the nanofluid buoyancy ratio,  $Nc$  is the regular double-diffusive buoyancy ratio,  $Nb$  is the Brownian motion parameter,  $Nt$  is the thermophoresis parameter,  $Nd$  is the modified Dufour parameter,  $Le$  is the usual Lewis number,  $Ld$  is the Dufour-contaminant Lewis number, and  $Ln$  is the nanofluid Lewis number, which are defined as

$$\begin{aligned}
 Re &= \frac{\rho_{f0} \bar{u}_{in} L}{\mu}, \quad Pr = \frac{\mu}{\rho_{f0} \alpha_m}, \quad Ra = \frac{(1 - \bar{\varphi}_{in}) g K \rho_{f0} \beta_T (T_h - T_{in}) L}{\alpha_m \mu}, \\
 Nr &= \frac{(\rho_p - \rho_{f0}) \bar{\varphi}_{in}}{\rho_{f0} \beta_T (T_h - T_{in}) (1 - \bar{\varphi}_{in})}, \\
 Nc &= \frac{\beta_C (\bar{C}_h - \bar{C}_{in})}{\beta_T (T_h - T_{in})}, \quad Ln = \frac{\alpha_m}{\varepsilon D_B}, \quad Nb = \frac{\delta D_B \bar{\varphi}_{in}}{\alpha_m}, \quad Nt = \frac{\delta D_T (T_h - T_{in})}{\alpha_m T_{in}}, \\
 Nd &= \frac{\sigma D_{TC} (\bar{C}_h - \bar{C}_{in})}{\alpha_m (T_h - T_{in})}, \\
 Le &= \frac{\alpha_m}{\varepsilon D_{Sm}}, \quad Ld = \frac{D_{CT} (T_h - T_{in})}{D_{Sm} (\bar{C}_h - \bar{C}_{in})}
 \end{aligned} \tag{24}$$

The physical quantities of interest are the local Nusselt  $Nu$  and Sherwood  $Sh, Sh_\varphi$  numbers along the right vertical wall, which are defined as

$$Nu = - \left( \frac{\partial \theta}{\partial x} \right)_{x=1}, \quad Sh = - \left( \frac{\partial C}{\partial x} \right)_{x=1}, \quad Sh_\varphi = - \left( \frac{\partial \varphi}{\partial x} \right)_{x=1} \tag{25}$$

and the average Nusselt  $\bar{Nu}$  and Sherwood  $\bar{Sh}, \bar{Sh}_\varphi$  numbers, which are given by

$$\bar{Nu} = \frac{1}{0.8} \int_0^{0.8} Nu \, dy, \quad \bar{Sh} = \frac{1}{0.8} \int_0^{0.8} Sh \, dy, \quad \bar{Sh}_\varphi = \frac{1}{0.8} \int_0^{0.8} Sh_\varphi \, dy \tag{26}$$

### 3 Numerical Method

The partial differential equations (19)–(22) with corresponding boundary conditions (23) were solved using the finite difference method with the second-order central differencing schemes (see Aleshkova and Sheremet 2010; Sheremet and Trifonova 2013; Sheremet et al. 2014; Sheremet and Pop 2014). The solution for the corresponding linear algebraic equations was obtained through the successive under relaxation method. Optimum value of the relaxation parameter was chosen on the basis of computing experiments. The computation is terminated when the residuals for the stream function get below  $10^{-7}$ .

For the purpose of obtaining grid independent solution, a grid sensitivity analysis was performed by preparing the solution for steady-state double-diffusive mixed convection in a square porous cavity filled with a Cu–water nanofluid at  $Re = 100, Pr = 0.2, Ra = 100, Nc = Nr = Nb = Nt = Nd = 0.1, Le = Ld = Ln = 1.0, \varepsilon = 0.9$ , solid matrix of the porous medium is the aluminum foam. Four cases of non-uniform grid are tested: a grid of  $100 \times 100$  points ( $\Delta x_{min} = \Delta y_{min} = 0.00087$  and  $\Delta x_{max} = \Delta y_{max} = 0.038$ ), a grid of  $150 \times 150$  points ( $\Delta x_{min} = \Delta y_{min} = 0.00022$  and  $\Delta x_{max} = \Delta y_{max} = 0.033$ ), a grid of  $200 \times 200$  points ( $\Delta x_{min} = \Delta y_{min} = 0.00019$  and  $\Delta x_{max} = \Delta y_{max} = 0.024$ ), and a grid

**Table 1** Variations of the average Nusselt and contaminant Sherwood numbers with the non-uniform grid

Non-uniform grids	$\overline{Nu}$	$\Delta = \frac{ \overline{Nu}_{i \times j} - \overline{Nu}_{200 \times 200} }{\overline{Nu}_{i \times j}}$	$\overline{Sh}_C$	$\Delta = \frac{ \overline{Sh}_{C i \times j} - \overline{Sh}_{C 200 \times 200} }{\overline{Sh}_{C i \times j}}$
		$\times 100\%$		$\times 100\%$
100×100	−4.784	1.53	−0.467	1.28
150×150	−4.716	0.11	−0.462	0.22
200×200	−4.711	–	−0.461	–
250×250	−4.709	0.04	−0.460	0.22

**Table 2** Comparison of the average Nusselt and Sherwood numbers

Ra	Le	Present results		Goyeau et al. (1996)		Bourich et al. (2004)	
		$\overline{Nu}$	$\overline{Sh}$	$\overline{Nu}$	$\overline{Sh}$	$\overline{Nu}$	$\overline{Sh}$
100	10	3.09	13.45	3.11	13.25	3.11	13.27
	20	3.09	19.34	3.11	18.89	3.11	19.02
200	10	4.96	20.37	4.96	19.86	4.96	20.02
	20	4.96	29.23	4.96	28.17	4.96	28.37
500	10	8.96	34.71	8.93	33.27	9.075	33.27
	20	8.96	47.58	8.93	46.77	9.075	45.91

of  $250 \times 250$  points ( $\Delta x_{\min} = \Delta y_{\min} = 0.00015$  and  $\Delta x_{\max} = \Delta y_{\max} = 0.0194$ ). Table 1 shows an effect of the mesh on the average Nusselt number of the right vertical wall.

On the basis of the conducted verifications, the non-uniform grid of  $200 \times 200$  points has been selected for the following analysis.

The numerical methodology was coded in C++, and to check its validity, a comparison with selective data from the published literature was carried out. The performance of the double-diffusive convection was tested against the results of Goyeau et al. (1996) and Bourich et al. (2004) for steady-state double-diffusive natural convection in a porous cavity differentially heated and salted. Table 2 shows the values of the average Nusselt and Sherwood numbers computed for various Rayleigh and Lewis numbers at  $Nc = 0$  in comparison with data of Goyeau et al. (1996) and Bourich et al. (2004).

It can be seen in Table 2 that the present mathematical model and numerical method are in good agreement with the earlier results for double-diffusive natural convection in a porous cavity. The performance of natural convection in a porous enclosure part of the model was tested earlier (see Sheremet et al. 2014; Sheremet and Pop 2014).

### 4 Results and Discussion

Numerical investigation of the boundary value problem (19)–(23) has been carried out at the following values of key parameters: Reynolds number ( $Re = 10–100$ ), Prandtl number ( $Pr = 0.2$ ), Rayleigh number ( $Ra = 50–500$ ), usual Lewis number ( $Le = 1–50$ ), Dufour-contaminant Lewis number ( $Ld = 1–50$ ), nanofluid Lewis number ( $Ln = 1–50$ ), nanofluid buoyancy ratio ( $Nr = 0.1–0.4$ ), regular double-diffusive buoyancy ratio ( $Nc =$



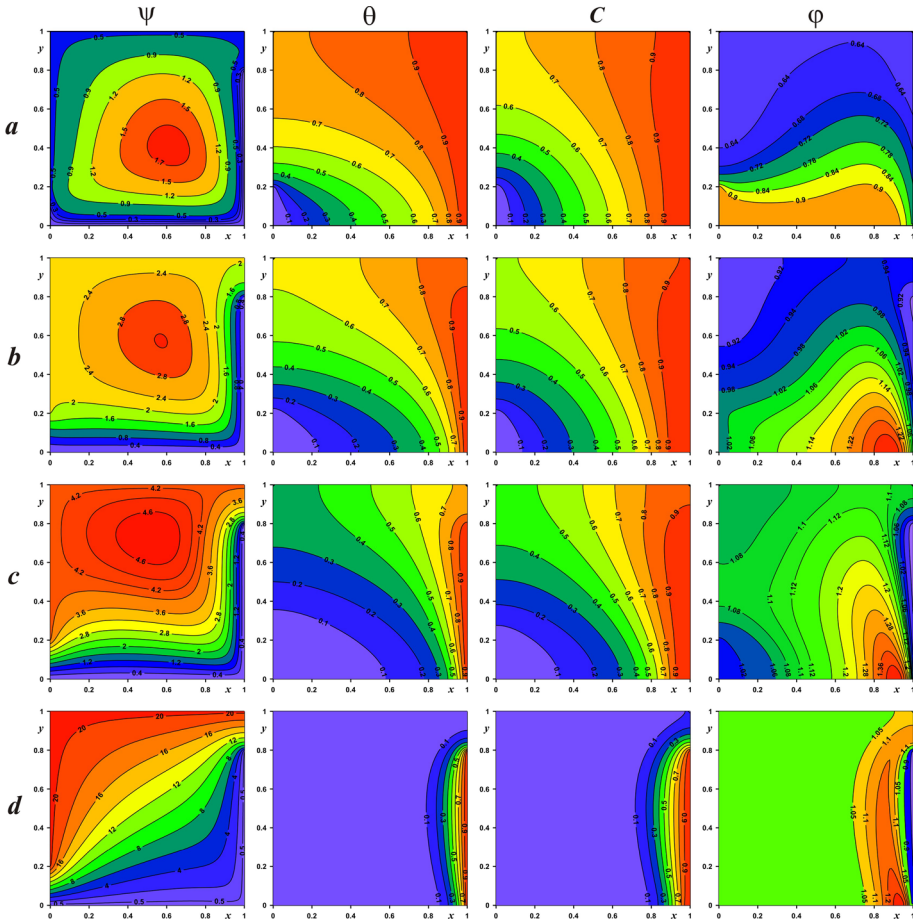


**Fig. 2** Streamlines  $\psi$ , isotherms  $\theta$ , isoconcentrations of contaminant  $C$ , and nanoparticles volume fraction  $\phi$  at  $Ra = 50, Le = Ld = Ln = 1.0, Nr = Nc = Nb = Nt = Nd = 0.1 : Re = 10 - a, Re = 50 - b, Re = 100 - c, Re = 500 - d$

0.1–0.4), Brownian motion parameter ( $Nb = 0.1–0.4$ ), the thermophoresis parameter ( $Nt = 0.1–0.4$ ), modified Dufour parameter ( $Nd = 0.1–0.4$ ). Particular efforts have been focused on the effects of these key parameters on the fluid flow, heat and mass transfer characteristics.

Figure 2 presents the effect of the Reynolds number on isolines of stream function, temperature, contaminant concentration and nanoparticles volume fraction at  $Ra = 50, Le = Ld = Ln = 1.0, Nr = Nc = Nb = Nt = Nd = 0.1$ .

It should be noted that an increase in the Reynolds number is related to an increase in the inlet velocity  $\bar{u}_{in}$ . Regardless of  $Re$  in the domain of interest, one can find a forced flow due to a presence of inlet and outlet and a single circulation flow due to the effect of the temperature and concentration differences between the right vertical wall and the fluid inside the cavity. Therefore, the considered modes are defined by the interaction of the forced flow and natural convection circulation. The presence of external forced flow leads to cooling of the domain of interest with a reduction in the contaminant concentration. Distributions of low temperature

and concentration wave from the inlet to outlet characterize the momentum transport in the same direction. An increase in the inlet velocity ( $Re \leq 100$ ) leads to an intensification of forced flow along the bottom wall and as a result the convective single circulation in the central part of the cavity. The latter is caused by an intensification of flow along interface between these flows. For high values of  $Re$ , the intensive forced flow is characterized by widening of the forced fluid tube. In case of  $Re = 500$  (Fig. 2d), the forced flow is a prevailing flow inside the cavity. Therefore, it is possible to conclude that for  $Re < 100$ , we have the natural convection mode, for  $100 \leq Re < 300$ , we have the mixed convection regime and for high values of the Reynolds number, we have the forced convection regime. It is worse noting that in case of the forced convection regime, the single circulation flow has small sizes or is absent. The average temperature and contaminant concentration inside the cavity are fully defined by the inlet conditions and confined the essential variations of  $\theta$  and  $C$  close to the right vertical wall.

Distributions of nanoparticles volume fraction are essentially non-homogeneous. An increase in the inlet velocity leads to homogenization of nanoparticles distribution inside the cavity. It should be noted that homogenization of nanoparticles distribution in case of the intensive circulation has been noticed early in the case of natural convection inside the three- and two-dimensional domains (see Sheremet et al. 2014; Sheremet and Pop 2014).

In Fig. 3, streamlines, isotherms, contaminant isoconcentrations, and nanoparticles isoconcentrations are presented for different values of the Rayleigh number at  $Re = 100$ ,  $Le = Ld = Ln = 1.0$ ,  $Nr = Nc = Nb = Nt = Nd = 0.1$ . Study of the Rayleigh number effect on the mixed convection processes within a porous medium is very important. For small values of the Rayleigh number ( $Ra = 50$ ), the forced convection is a prevailing heat transfer mode with heat and mass conduction regime. The latter is clearly presented in the temperature and concentration fields close to the right vertical wall. The isotherms and isoconcentrations are parallel to each other close to this wall. The flow inside the cavity is characterized only by external forced flow without any recirculation. At the same time, a penetration of the cold temperature and low contaminant concentration for this regime is more essential in comparison with other one. An increase in the Rayleigh number to the value  $Ra = 50$  (Fig. 2c) leads to a formation of the single recirculation in the central part of the cavity that distorts the forced flow and reduces the penetration of the low temperature and contaminant concentration into the cavity. Further increase in  $Ra$  leads to a formation of central convective vortex of high intensity that essentially confines external forced flow. Distributions of nanoparticles characterize the developed hydrodynamic and temperature field.

The effect of the Reynolds and Rayleigh numbers on the average Nusselt and contaminant Sherwood numbers at right vertical wall for  $Le = Ld = Ln = 1.0$ ,  $Nr = Nc = Nb = Nt = Nd = 0.1$  is presented in Fig. 4. Taking into account boundary conditions for the nanoparticles volume fraction (23) dependences of  $\overline{Sh}_\varphi$  are similar to Fig. 4a.

An increase in  $Re$  from 10 to 500 leads to an essential increase in  $|\overline{Nu}|$  and  $|\overline{Sh}|$  due to the heat and contaminant removal from the vertical wall. An increase in the Rayleigh number also leads to an increase in  $|\overline{Nu}|$  with non-monotonic changes of  $|\overline{Sh}|$ . It should be noted that an increase in the Rayleigh number from 100 to 400, one can find a reduction in  $|\overline{Sh}|$  and the following increase in  $Ra$  leads to an increase in  $|\overline{Sh}|$ . Such behavior can be explained by thermo diffusion effect.

Figure 5 shows an effect of the usual Lewis number on the average Nusselt and contaminant Sherwood numbers. An increase in  $Le$  leads to an essential intensification of convective mass transfer and attenuation of convective heat transfer, namely  $|\overline{Sh}|$  increases while  $|\overline{Nu}|$  and

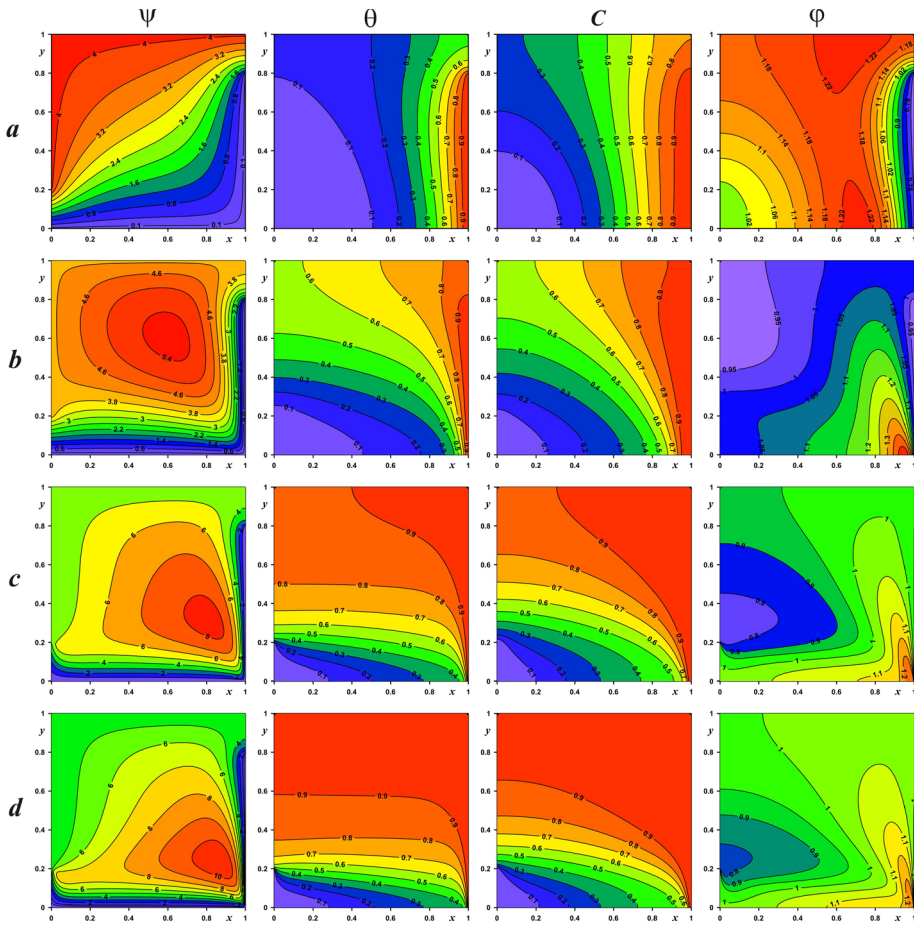


**Fig. 3** Streamlines  $\psi$ , isotherms  $\theta$ , isoconcentrations of contaminant  $C$ , and nanoparticles volume fraction  $\varphi$  at  $Re = 100, Le = Ld = Ln = 1.0, Nr = Nc = Nb = Nt = Nd = 0.1:Ra = 10 - a, Ra = 100 - b, Ra = 500 - c, Ra = 1000 - d$

$|\overline{Sh}_\varphi|$  decrease (e.g., an increase in  $Le$  from 1.0 to 10.0 at  $Ra = 50, Re = 100.0$  leads to both a reduction in  $|\overline{Nu}|$  up to 42% and an increment in  $|\overline{Sh}|$  in 30 times).

The effects of the Brownian motion and thermophoresis parameters on the average Nusselt and contaminant Sherwood numbers are presented in Figs. 6 and 7. An increase in the Brownian motion parameter leads to an insignificant decrease in  $|\overline{Nu}|$  and an inessential increase in  $|\overline{Sh}|$  (see Fig. 6). At the same time, an increase in the thermophoresis parameter from 0.1 to 0.4 leads to insignificant nonlinear changes of  $|\overline{Nu}|$ , namely for  $Re < 90$ , one can find an inessential reduction in convective heat transfer, for  $100 < Re < 200$  one can find an inessential intensification of convective heat transfer and for  $Re > 300$ , we have also an attenuation of convective heat transfer. Changes of the average contaminant Sherwood numbers with  $Nt$  are nonlinear. An increase in  $Nt$  leads to an insignificant intensification of convective mass transfer for  $Re < 90$ , a reduction in  $|\overline{Sh}|$  for  $90 < Re < 500$  and also intensification of convective mass transfer for  $Re > 500$ .

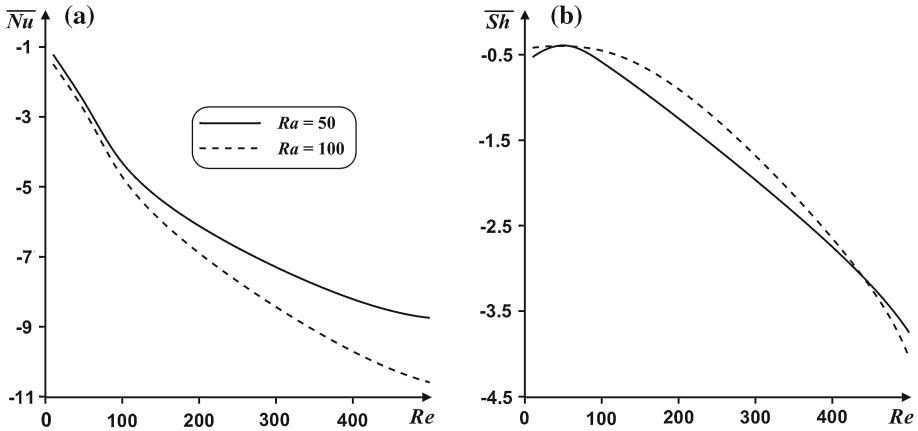


**Fig. 4** Variation of the average Nusselt (a) and Sherwood (b) numbers at right vertical wall with different Reynolds and Rayleigh numbers for  $Le = Ld = Ln = 1.0, Nr = Nc = Nb = Nt = Nd = 0.1$

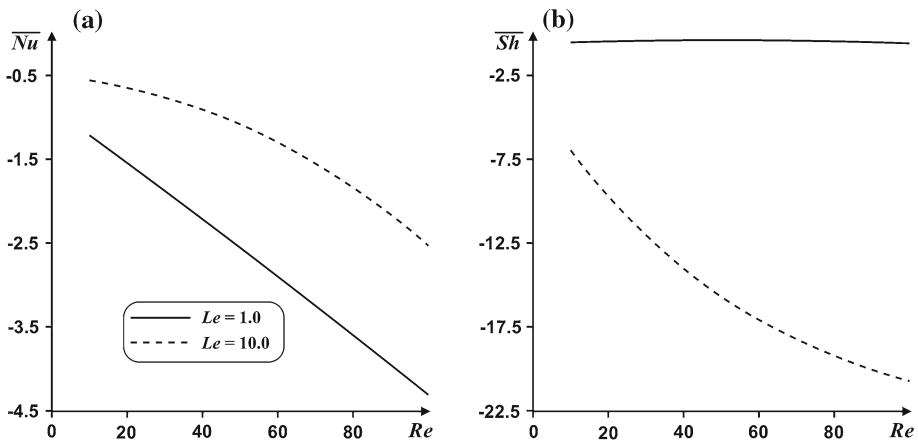


**Fig. 5** Variation of the average Nusselt (a) and Sherwood (b) numbers at right vertical wall with different Reynolds and usual Lewis numbers for  $Ra = 50, Ld = Ln = 1.0, Nr = Nc = Nb = Nt = Nd = 0.1$

### 5 Conclusions

Double-diffusive mixed convection in a porous cavity with one isothermal vertical wall filled with a nanofluid has been numerically studied. Particular efforts have been focused on the effects of the Rayleigh, Reynolds and usual Lewis numbers, Brownian motion and thermophoresis parameters on flow field, temperature, contaminant and nanoparticles volume fraction distributions, and average Nusselt and Sherwood numbers. It has been found that the average Nusselt number at hot vertical wall is an increasing function of the Rayleigh and Reynolds numbers and a decreasing function of the usual Lewis number. While the average Sherwood number at this vertical wall is an increasing function of the usual Lewis. Effects of the Rayleigh and Reynolds numbers on  $|\overline{Sh}|$  and the thermophoresis parameter on the average Nusselt and Sherwood numbers are non-monotonic. It has been shown that in the present

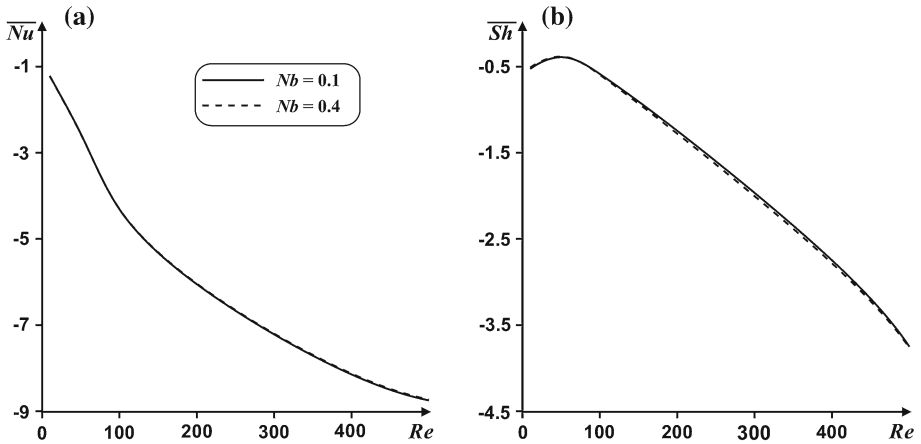


**Fig. 6** Variation of the average Nusselt (a) and Sherwood (b) numbers at right vertical wall with different Reynolds and Brownian motion parameter for  $Ra = 50, Le = Ld = Ln = 1.0, Nr = Nc = Nt = Nd = 0.1$

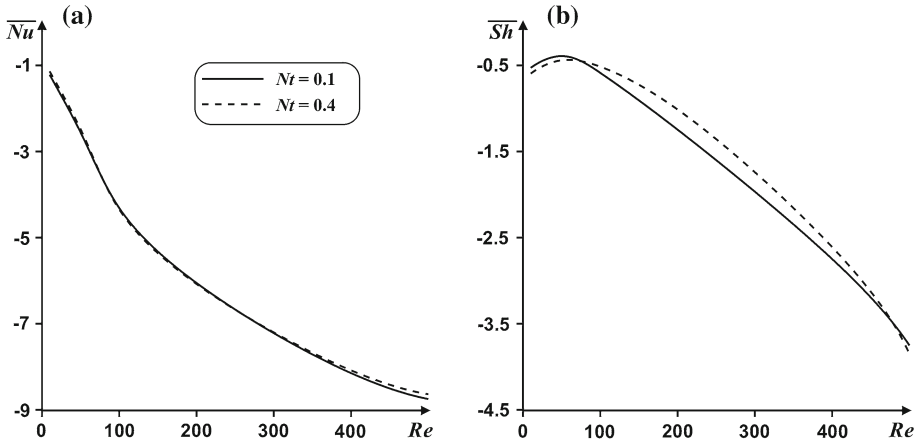


**Fig. 7** Variation of the average Nusselt (a) and Sherwood (b) numbers at right vertical wall with different Reynolds and thermophoresis parameter for  $Ra = 50, Le = Ld = Ln = 1.0, Nr = Nc = Nb = Nd = 0.1$

porous problem, the Richardson number  $Ri = Gr/Re^2$  does not define the prevailing of the forced or natural convection modes. For example, at  $Ra = 500$  and  $Re = 100$  (Fig. 3c), we have the natural convection regime with essential central circulation while  $Ri = 0.25 < 1$ .

**Acknowledgments** This work of M.A. Sheremet was conducted as a government task of the Ministry of Education and Science of the Russian Federation, Project Number 13.1919.2014/K. The authors wish also to express their thank to the very competent Reviewers for the valuable comments and suggestions. They also thanks to Dr. T. Grosan for the important suggestions.

**References**

Abib, A.H., Jaluria, Y.: Numerical simulation of the buoyancy-induced flow in a partially open enclosure. *Numer. Heat Transf.* **14**, 235–254 (1988)

- Aleshkova, I.A., Sheremet, M.A.: Unsteady conjugate natural convection in a square enclosure filled with a porous medium. *Int. J. Heat Mass Transf.* **53**, 5308–5320 (2010)
- Bachok, N., Ishak, A., Pop, I.: Stagnation-point flow over a stretching/shrinking sheet in a nanofluid. *Nanoscale Res. Lett.* **6**, 10 (2011)
- Bennacer, R., Tobbal, A., Beji, H., Vasseur, P.: Double diffusive convection in a vertical enclosure filled with anisotropic porous media. *Int. J. Therm. Sci.* **40**, 30–41 (2001)
- Bilgen, E., Oztop, H.: Natural convection heat transfer in partially open inclined square cavities. *Int. J. Heat Mass Transf.* **48**, 1470–1479 (2005)
- Bourich, M., Hasnaoui, M., Amahmid, A.: Double-diffusive natural convection in a porous enclosure partially heated from below and differentially salted. *Int. J. Heat Fluid Flow* **25**, 1034–1046 (2004)
- Buongiorno, J.: Convective transport in nanofluids. *ASME J. Heat Transf.* **128**, 240–250 (2006)
- Chamkha, A.J., Al-Naser, H.: Double-diffusive convection in an inclined porous enclosure with opposing temperature and concentration gradients. *Int. J. Therm. Sci.* **40**, 227–244 (2001)
- Costa, V.A.F.: Double-diffusive natural convection in parallelogrammic enclosures filled with fluid-saturated porous media. *Int. J. Heat Mass Transf.* **47**, 2699–2714 (2004a)
- Costa, V.A.F.: Double-diffusive natural convection in parallelogrammic enclosures. *Int. J. Heat Mass Transf.* **47**, 2913–2926 (2004b)
- Davarzani, H., Marcoux, M., Quintard, M.: Theoretical predictions of the effective thermodiffusion coefficients in porous media. *Int. J. Heat Mass Transf.* **53**, 1514–1528 (2010)
- De Groot, S.R., Mazur, P.: *Non-equilibrium Thermodynamics*. Dover, New York (1984)
- Firoozabadi, A.: *Thermodynamics of Hydrocarbon Reservoirs*. McGraw-Hill, New York (1991)
- Goyeau, B., Songbe, J.-P., Gobin, D.: Numerical study of double-diffusive natural convection in a porous cavity using the Darcy–Brinkman formulation. *Int. J. Heat Mass Transf.* **39**, 1363–1378 (1996)
- Ilya, I.R.: On double diffusive convection with Soret effect in a vertical layer between co-axial cylinders. *Phys. D* **215**, 191–200 (2006)
- Jaimala, Singh, R.: A note on the paper of Nield and Kuznetsov. *Transp. Porous Media* **102**, 137–138 (2014)
- Jeng, D.Z., Yang, C.S., Gau, C.: Experimental and numerical study of transient natural convection due to mass transfer in inclined enclosures. *Int. J. Heat Mass Transf.* **52**, 181–192 (2009)
- Kaviany, M.: *Principles of Heat Transfer in Porous Media*, 2nd edn. Springer, New York (1999)
- Karimi-Fard, M., Charrier-Mojtabi, M.C., Vafai, K.: Non-Darcian effects on double-diffusive natural convection within a porous medium. *Numer. Heat Transf. Part A* **30**, 837–851 (1997)
- Khan, A.V., Pop, I.: Boundary-layer flow of a nanofluid past a stretching sheet. *Int. J. Heat Mass Transf.* **53**, 2477–2483 (2010)
- Khanafar, K., Vafai, K., Lightstone, M.: Buoyancy-driven heat transfer enhancement in a two-dimensional enclosure utilizing nanofluids. *Int. J. Heat Mass Transf.* **46**, 3639–3653 (2003)
- Kuznetsov, A.V., Nield, D.A.: Double-diffusive natural convective boundary-layer flow of a nanofluid past a vertical plate. *Int. J. Therm. Sci.* **50**, 712–717 (2011)
- Kuznetsov, A.V., Nield, D.A.: The Cheng–Minkowycz problem for natural convective boundary layer flow in a porous medium saturated by a nanofluid: A revised model. *Int. J. Heat Mass Transf.* **65**, 682–685 (2013)
- Mansour, M.A., Abd-Elaziz, M.M., Mohamed, R.A., Ahmed, S.E.: Unsteady natural convection, heat and mass transfer in inclined triangular porous enclosures in the presence of heat source or sink: effect of sinusoidal variation of boundary conditions. *Transp. Porous Media* **87**, 7–23 (2011)
- Mohamad, A.A.: *Natural convection in open cavities and slots*. *Numer. Heat Transf. Part A* **27**, 705–716 (1995)
- Nakayama, A.: *PC-Aided Numerical Heat Transfer and Convective Flow*. CRC Press, Boca Raton (1995)
- Nield, D.A., Bejan, A.: *Convection in Porous Media*, 4th edn. Springer, New York (2013)
- Nield, D.A., Kuznetsov, A.V.: The Cheng–Minkowycz problem for the double-diffusive natural convective boundary layer flow in a porous medium saturated by a nanofluid. *Int. J. Heat Mass Transf.* **54**, 374–378 (2011)
- Nield, D.A., Kuznetsov, A.V.: The effect of vertical throughflow on thermal instability in a porous medium layer saturated by a nanofluid: a revised model. *ASME J. Heat Transf.* **137**, 052601 (2015)
- Nithiarasu, P., Sundararajan, T., Seetharamu, K.N.: Double-diffusive natural convection in a fluid saturated porous cavity with a freely convecting wall. *Int. Commun. Heat Mass Transf.* **24**, 1121–1130 (1997)
- Rabinovich, G.D.: *Separation of Isotopes and Other Mixtures by Thermal Diffusion*. Atomizdat, Moscow (1981)
- Rashad, A.M., Ahmed, S.E., Mansour, M.A.: Effects of chemical reaction and thermal radiation on unsteady double diffusive convection. *Int. J. Numer. Methods Heat Fluid Flow* **24**, 1124–1140 (2014)
- Saleh, H., Hashim, I.: Conjugate natural convection in an open-ended porous square cavity. *J. Porous Media* **16**, 291–302 (2013)

- Schaefer, H.-E.: *Nanoscience: The Science of the Small in Physics, Engineering, Chemistry, Biology and Medicine*. Springer, New York (2010)
- Sheremet, M.A., Trifonova, T.A.: Unsteady conjugate natural convection in a vertical cylinder partially filled with a porous medium. *Numer. Heat Transf. Part A* **64**, 994–1015 (2013)
- Sheremet, M.A., Grosan, T., Pop, I.: Free convection in shallow and slender porous cavities filled by a nanofluid using Buongiorno's model. *ASME J. Heat Transf.* **136**, 082501 (2014)
- Sheremet, M.A., Pop, I.: Conjugate natural convection in a square porous cavity filled by a nanofluid using Buongiorno's mathematical model. *Int. J. Heat Mass Transf.* **79**, 137–145 (2014)
- Wiegand, S.: Thermal diffusion in liquid mixtures and polymer solutions. *J. Phys. Condens. Matter* **16**, 357–379 (2004)